

Monitoring squeezed collective modes of a 1D Bose gas after an interaction quench using density ripples analysis : Supplementary Material

Max Schemmer¹, Aisling Johnson¹, and Isabelle Bouchoule¹

¹Laboratoire Charles Fabry, Institut d'Optique, CNRS, Université Paris Sud 11, 2 Avenue Augustin Fresnel, F-91127 Palaiseau Cedex, France

January 8, 2018

This Supplementary Material gives technical information and details of calculations related to our paper entitled “Monitoring squeezed collective modes of a 1D Bose gas after an interaction quench using density ripples analysis” (arXiv:1712.04642), referred to as the “main text”. In the first section we give a general derivation of the density ripples power spectrum, which does not *a priori* assume a homogeneous system. The second section gives the result for a homogeneous system and the analytical prediction for thermal equilibrium¹. The third section details the derivation of the density ripples power spectrum for a trapped gas, computed using the results for homogeneous gases and the local density approximation. The fourth section provides the explicit calculation of the post-quench evolution of the power spectrum for a harmonically trapped gas, namely the calculation of the function \mathcal{F} of the main text. In the fifth section, we verify the validity of the local density approximation for the parameters of the data presented in the main text. For this purpose, we compute the density ripple power spectrum using the Bogoliubov modes of the trapped gas. In the sixth section, we justify that interactions play a negligible role during time-of-flight, so that the calculations of the density ripples power spectrum, which assume instantaneous switch-off of the interactions, are valid. In the seventh section, we investigate two effects that are responsible for a reduction of the oscillation amplitude of the quantity $\bar{J}(\tau)$, extracted from the data, as compared to the simple theoretical predictions Eq. (6) of the main text : First the finite ramp time of the interaction strength decreases the squeezing of the collective modes, and second the finite resolution in τ resulting from data binning is responsible for a decrease of the expected oscillation amplitude on the processed data.

1 Derivation of the density ripples power spectrum

The power spectrum of density ripples has been first investigated in the limit of small density ripples and for a gas initially in the 3D Thomas-Fermi regime (*i.e.* $\mu \gg \hbar\omega_{\perp}$) [2, 3]. It was then computed assuming instantaneous switch off of the interactions in [1]. Here, for consistency, we rederive Eq. (4) and (5) of the main text. Since we will later be interested in trapped gases, let us first assume a general case where we do not *a priori* assume a homogeneous system. We let the gas evolve freely for a time t_f after interactions have been switched off. The power spectrum of the density

¹We corrected the formula published in [1]

fluctuations after t_f writes

$$\langle |\tilde{\rho}(q)|^2 \rangle = \int \int dz_1 dz_2 e^{iq(z_1 - z_2)} \langle \delta n(z_1, t_f) \delta n(z_2, t_f) \rangle. \quad (\text{SM1})$$

Writing $\delta n(z) = n(z) - \langle n(z) \rangle$ and expanding the above equation, the term $|\int dz e^{iqz} \langle n(z, t_f) \rangle|^2$ appears. Here we consider times of flight short enough so that the shape of the cloud barely changes during time of flight, so that $\langle n(z, t_f) \rangle \simeq \langle n(z, 0) \rangle$. We moreover consider wavevectors q much larger than the inverse of the cloud length, such that $|\int dz e^{iqz} \langle n(z, 0) \rangle|^2$ is a negligible quantity. We then have

$$\langle |\tilde{\rho}(q)|^2 \rangle \simeq \int \int dz_1 dz_2 e^{iq(z_1 - z_2)} \langle n(z_1, t_f) n(z_2, t_f) \rangle. \quad (\text{SM2})$$

To compute $n(z, t_f) = \Psi^+(z, t_f) \Psi(z, t_f)$ we evolve the atomic field with its free propagator, which leads to

$$\psi(z, t_f) = \frac{1}{\sqrt{2\pi t_f}} \int d\alpha \psi(\alpha, 0) e^{i\frac{(z-\alpha)^2}{2t_f}}, \quad (\text{SM3})$$

where for simplicity we use a unit system in which $m = \hbar = 1$. We then have

$$\langle n(z_1, t_f) n(z_2, t_f) \rangle = \frac{1}{(2\pi t_f)^2} \int \int \int d\alpha d\beta d\gamma d\delta \langle \psi_\alpha^+ \psi_\beta \psi_\gamma^+ \psi_\delta \rangle e^{-i\frac{(z_1-\alpha)^2}{2t_f}} e^{i\frac{(z_1-\beta)^2}{2t_f}} e^{-i\frac{(z_2-\gamma)^2}{2t_f}} e^{i\frac{(z_2-\delta)^2}{2t_f}}, \quad (\text{SM4})$$

where we use the simplified notation $\psi_\nu = \psi(\nu, 0)$. Expanding the exponentials, the above expression writes

$$\langle n(z_1, t_f) n(z_2, t_f) \rangle = \frac{1}{(2\pi t_f)^2} \int \int \int d\alpha d\beta d\gamma d\delta \langle \psi_\alpha^+ \psi_\beta \psi_\gamma^+ \psi_\delta \rangle e^{i\frac{(\alpha-\beta)z_1}{t_f}} e^{i\frac{\beta^2-\alpha^2}{2t_f}} e^{i\frac{(\gamma-\delta)z_2}{t_f}} e^{i\frac{\delta^2-\gamma^2}{2t_f}}. \quad (\text{SM5})$$

Injecting into Eq. (SM2), and using $\int dz e^{ikz} = 2\pi\delta(k)$ and $\delta(x/\alpha) = \alpha\delta(x)$, we get

$$\langle |\tilde{\rho}(q)|^2 \rangle = \int \int d\alpha d\delta \langle \psi_\alpha^+ \psi_{\alpha+qt_f} \psi_{\delta+qt_f}^+ \psi_\delta \rangle e^{-i\frac{\alpha^2}{2t_f}} e^{i\frac{(\alpha+qt)^2}{2t_f}} e^{-i\frac{(\delta+qt)^2}{2t_f}} e^{i\frac{\delta^2}{2t_f}}. \quad (\text{SM6})$$

Doing the variable change $\delta = \alpha + X$ we obtain, after some algebra,

$$\langle |\tilde{\rho}(q)|^2 \rangle = \int \int d\alpha dX e^{iqX} \langle \psi_\alpha^+ \psi_{\alpha+qt_f} \psi_{\alpha+X+qt_f}^+ \psi_{\alpha+X} \rangle. \quad (\text{SM7})$$

For gases lying deep into the quasi-condensate regime, one can neglect density fluctuations when estimating the expectation value in the above equation, such that

$$\langle |\tilde{\rho}(q)|^2 \rangle \simeq \int \int d\alpha dX e^{iqX} \sqrt{n(\alpha)n(\alpha+qt_f)n(\alpha+X+qt_f)n(\alpha+X)} \langle e^{i(\theta(\alpha)-\theta(\alpha+qt_f)+\theta(\alpha+X+qt_f)-\theta(\alpha+X))} \rangle. \quad (\text{SM8})$$

The following section applies this result to homogeneous systems. This equation is however not restricted to homogeneous systems and we will use it to treat the effect of the trap beyond the local density approximation.

2 Power spectrum of the density ripples for a homogeneous gas

For a homogeneous gas, the relevant quantity is an intensive variable which relates to the expression $\langle |\tilde{\rho}(q)|^2 \rangle$ of the previous section by

$$\langle |\rho(q)|^2 \rangle = \frac{1}{L} \langle |\tilde{\rho}(q)|^2 \rangle \quad (\text{SM9})$$

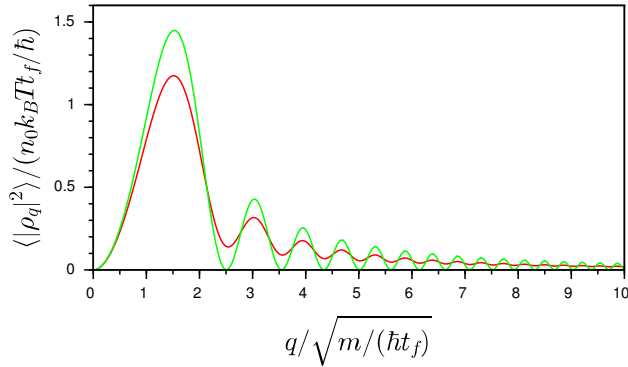


Figure 1: Density ripples power spectrum for a homogeneous gas. The exact formula Eq. (SM11) (red curve) is compared to the small q approximation given Eq. (5) of the main text, where $\langle |\rho(q)|^2 \rangle$ is proportional to $\langle \theta_q^2 \rangle$ (green curve). The only relevant parameter is $\hbar t_f / (m l_c^2)$. Calculations shown correspond to $\hbar t_f / (m l_c^2) = 0.05$, a value corresponding to the data shown in Fig. (2,b) of the main text, the correlation length $l_c = 2\hbar^2 n_0 / (m k_B T)$ being computed for the central density.

where L is the length of the box used for the calculation. Injecting Eq. (SM8) into Eq. (SM9), we recover Eq. (3) and (4) of the main text, up to an irrelevant term in $\delta(q)$ (see footnote²). In fact, we can use the Wick theorem, which one can apply since θ is a Gaussian variable³, to obtain

$$\langle |\rho(q)|^2 \rangle = n_0^2 \int dX e^{iqX} e^{-\frac{1}{2} \langle (\theta(0) - \theta(qt_f) + \theta(X+qt_f) - \theta(X))^2 \rangle}. \quad (\text{SM10})$$

To compute the power spectrum of density ripples for a thermal equilibrium state, we follow the calculation made in [1] and expand the exponential term in Eq. (SM10) as a function of the first order correlation function $g^{(1)}(z) = n_0 e^{-\frac{1}{2} \langle (\theta(0) - \theta(z))^2 \rangle}$, which fulfils $g^{(1)}(z) = n_0 e^{-|z|/l_c}$ where $l_c = 2\hbar^2 n_0 / (k_B T)$ [1]. Calculation of the integral in Eq. (SM10) then leads to

$$\langle |\rho(q)|^2 \rangle = 2n_0^2 \frac{2ql_c - 2e^{-2\hbar q t_f / (m l_c)} (ql_c \cos(\hbar q^2 t_f / m) + 2 \sin(\hbar q^2 t_f / m))}{q(4 + l_c^2 q^2)}. \quad (\text{SM11})$$

Note that we corrected the formula given in [1]. The power spectrum computed with this equation is compared in Fig. 1 to the approximated formula valid for small q , namely Eq. (5) of the main text.

3 Density ripple spectrum for a harmonically confined gas under the Local Density Approximation (LDA)

Let us investigate the density ripples power spectrum in the case of a gas trapped in a longitudinal potential smooth enough so that the cloud size L is much larger than the typical phase correlation length l_c and much larger than

²This term is due to the approximation made when going from Eq. (SM1) to Eq. (SM2), which is valid only for q values larger than the inverse of the cloud size.

³The Hamiltonian being quadratic in θ , the distribution of θ is Gaussian at thermal equilibrium. The squeezing of each collective mode produced by the interaction quench preserves the Gaussian nature of θ .

$\hbar q t_f / m$: $L \gg l_c, \hbar q t_f / m$. As in section 1, we moreover consider the power spectrum only for wavevectors $q \gg 1/L$. Let us start with the general expression Eq. (SM1) that we write

$$\langle |\tilde{\rho}(q)|^2 \rangle = \int dz \int du \langle \delta\rho(z, t_f) \delta\rho(z + u, t_f) \rangle e^{iq u}. \quad (\text{SM12})$$

Let us consider $\langle \delta\rho(z, t_f) \delta\rho(z + u, t_f) \rangle$ for a given z . It decreases to 0 over a length much smaller than L , such that values of u significantly contributing significantly to the integral are much smaller than L . Moreover the region of the initial cloud contributing most to $\langle \delta\rho(z, t_f) \delta\rho(z + u, t_f) \rangle$ is much smaller than L for sufficiently large L . Then, to compute $\langle \delta\rho(z, t_f) \delta\rho(z + u, t_f) \rangle$ one can perform a local density approximation and use the result of a homogeneous gas at a density $n_0(z)$. We then obtain

$$\langle |\tilde{\rho}(q)|^2 \rangle = \int dz \langle |\rho_{n_0(z)}(q)|^2 \rangle \quad (\text{SM13})$$

where the subscript $n_0(z)$ specifies that one considers the result for an homogeneous gas at a density $n_0(z)$. This expression is referred to as the Local Density Approximation expression of the power spectrum. We have tested this approximation, for conditions close to the experimental data presented in the main text, by comparing it with calculations based on the Bogoliubov excitations of the trapped system (see section 5).

4 Evolution of the density ripple power spectrum for a harmonically confined gas under the LDA

Here we give an explicit derivation of Eq. (6) of main text, for a gas harmonically confined in a longitudinal trap of frequency ω_{\parallel} . Injecting into Eq. (SM13) Eq. (5) and Eq. (2) of the main text, and using the local initial power spectrum of θ which writes $\langle \theta_q^2 \rangle = mk_B T / (\hbar^2 n_0 q^2)$, we obtain Eq. (6) of the main text with

$$\mathcal{F} = \int dz n_0(z) \sin^2(c(z)qt) / N \quad (\text{SM14})$$

where N is the total atom number. The density profile $n_0(z)$ is estimated itself within the LDA, using the local chemical potential

$$\mu(z) = \mu_p (1 - (z/R_{\text{TF}})^2), \quad (\text{SM15})$$

where R_{TF} is the Thomas-Fermi radius of the density profile and μ_p is the chemical potential at the trap center. For a transverse harmonic confinement of frequency ω_{\perp} , it has been checked by comparison with predictions of the 3D Gross-Pitaevskii equation that the equation of state of the gas is very well described by the heuristic formula [4]

$$\mu(n) = \hbar\omega_{\perp} (\sqrt{1 + 4na} - 1), \quad (\text{SM16})$$

where a is the 3D scattering length between atoms. For small linear densities, we recover the 1D expression $\mu = 2\hbar\omega_{\perp} a n$, valid far from the confinement-induced resonance [5]. Using Eq. (SM16) and Eq. (SM15), we obtain the density profile

$$n_0(z) = \left[(\eta(1 - \tilde{z}^2) + 1)^2 - 1 \right] / (4a) \quad (\text{SM17})$$

where we introduced $\tilde{z} = z/R_{\text{TF}}$ and $\eta = \mu_p / (\hbar\omega_{\perp})$. This yields $N = (4/3\eta + 8\eta^2/15)R_{\text{TF}}/(2a)$. The local speed of sound on the other hand, obtained from the thermodynamic relation $c = \sqrt{n(\partial\mu/\partial n)/m}$, writes

$$c(z) = c_p \sqrt{\frac{(1 + \eta) \left[(1 + \eta(1 - \tilde{z}^2))^2 - 1 \right]}{(1 + \eta(1 - \tilde{z}^2)) ((1 + \eta)^2 - 1)}}, \quad (\text{SM18})$$

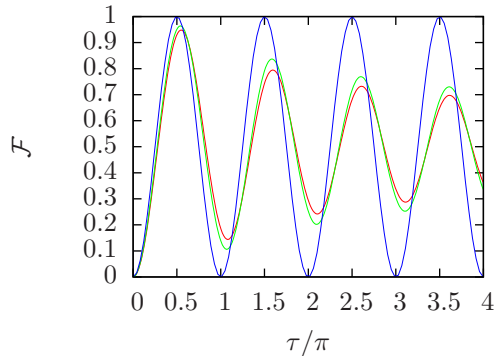


Figure 2: Oscillation of each spectral component of the power spectrum for a harmonically confined gas in the LDA. The function \mathcal{F} is shown in green, for $\eta = \mu_p/(\hbar\omega_\perp) = 1.0$. The pure 1D limit, corresponding to $\eta \ll 1$ is shown in red. The oscillations expected for a homogeneous gas are shown in blue. In all the cases, $\tau = cqt$ where c is the central sound velocity.

where c_p is the speed of sound computed for the central density. Injecting into Eq. (SM14), we then find

$$\mathcal{F} = \frac{1}{4\eta/3 + 8\eta^2/15} \int_0^1 d\tilde{z} \left[(1 + \eta(1 - \tilde{z}^2))^2 - 1 \right] \sin^2 \left(\tau \sqrt{\frac{(1 + \eta) \left[(1 + \eta(1 - \tilde{z}^2))^2 - 1 \right]}{(1 + \eta(1 - \tilde{z}^2)) ((1 + \eta)^2 - 1)}} \right). \quad (\text{SM19})$$

When the gas is deeply in the 1D regime, namely for $\eta \ll 1$, this expression reduces to

$$\mathcal{F}_{1\text{D}} = \frac{3}{2} \int_0^1 d\tilde{z} (1 - \tilde{z}^2) \sin^2 \left(\tau \sqrt{1 - \tilde{z}^2} \right). \quad (\text{SM20})$$

Experimentally, values of η are in the range [0.6; 1.3]. Fig. 2 shows the function \mathcal{F} , computed for $\eta = 1$. We compare it to $\mathcal{F}_{1\text{D}}$ and to the expression expected for a homogeneous gas, namely $\sin^2(\tau)$.

5 Beyond the Local density approximation: calculation using Bogoliubov modes of a harmonically confined 1D gas

We consider here a 1D gas confined longitudinally in a harmonic trap of frequency ω_\parallel . In opposition to the calculations done in the previous section we do not rely on the Local Density Approximation but use the Bogoliubov modes of the trapped gas to compute the post-quench evolution and the density ripples power spectrum. The relevant collective modes lie deep in the phononic regime. The Bogoliubov modes, indexed by an integer ν , then acquire an analytical dispersion relation and analytical wavefunctions that one can use for calculations. For each mode, the dynamics is accounted for by the harmonic oscillator Hamiltonian

$$H_\nu = \hbar\omega_\nu \left(\frac{x_\nu^2}{2} + \frac{p_\nu^2}{2} \right), \quad (\text{SM21})$$

where $\omega_\nu = \omega_{\parallel} \sqrt{\nu(\nu+1)/2}$ and x_ν and p_ν are canonically conjugate variables. The phase and density fluctuation operators write

$$\begin{cases} \theta(z) = \sum_\nu \theta_\nu(z) p_\nu \\ \delta n(z) = \sum_\nu n_\nu(z) x_\nu \end{cases} \quad (\text{SM22})$$

where

$$\begin{cases} \theta_\nu(z) = \frac{1}{\sqrt{2}} \left(\frac{mg}{\hbar^2 n_p} \right)^{1/4} \frac{\sqrt{2\nu+1}}{(\nu(\nu+1))^{1/4}} P_\nu(z/R_{TF}) \\ n_\nu(z) = \frac{\sqrt{2\nu+1}}{2R_{TF}} (\nu(\nu+1))^{1/4} \left(\frac{\hbar^2 n_p}{mg} \right)^{1/4} P_\nu(z/R_{TF}). \end{cases} \quad (\text{SM23})$$

Here n_p and R_{TF} are the central density and radius of the Thomas-Fermi profil $n_0(z) = n_p(1 - (z/R_{TF})^2)$. The interaction quench consists in changing the interaction strength, g going from g_i to $g_f = (1 + \kappa)g_i$ at $t = 0$, while changing the longitudinal oscillation frequency by a factor $\sqrt{1 + \kappa}$ so that R_{TF} stays constant. Then the interaction quench preserves the shapes of the wave functions θ_ν and n_ν , and it simply changes the canonical variables x_ν and p_ν according to

$$\begin{cases} x_\nu(t = 0^+) = (g_f/g_i)^{1/4} x_\nu(t = 0^-) \\ p_\nu(t = 0^+) = (g_i/g_f)^{1/4} p_\nu(t = 0^-) \end{cases} \quad (\text{SM24})$$

Under such a transformation, the initial thermal state, an isotropic Gaussian, becomes a squeezed state and the subsequent evolution under the Hamiltonian Eq. (SM21) leads to a breathing of each quadrature. In particular

$$\langle p_\nu^2 \rangle = \langle p_\nu^2 \rangle_i (1 + \kappa \sin^2(\omega_\nu t)). \quad (\text{SM25})$$

The initial value $\langle p_\nu^2 \rangle_i$ is given by the thermal expectation value, which reduces to

$$\langle p_\nu^2 \rangle_i = k_B T / (\hbar \omega_\nu) \quad (\text{SM26})$$

for the low-lying modes for which $k_B T \gg \hbar \omega_\nu$.

Let us now go back to the evolution of the density ripples. Injecting Eq. (SM22) into Eq. (SM8), using Wick theorem and the fact that different modes are uncorrelated we get

$$\langle |\tilde{\rho}(q)|^2 \rangle = \int \int d\alpha dX e^{iqX} \frac{\sqrt{n_0(\alpha)n_0(\alpha+qt_f)n_0(\alpha+X+qt_f)n_0(\alpha+X)}}{e^{-\frac{1}{2} \sum_\nu \langle p_\nu^2 \rangle (\theta_\nu(\alpha) - \theta_\nu(\alpha+qt_f) + \theta_\nu(\alpha+X+qt_f) - \theta_\nu(\alpha+X))^2}} \quad (\text{SM27})$$

For $\hbar qt_f/m \ll l_c$, where l_c is the correlation length of the phase, one can expand the exponential and $\langle |\tilde{\rho}(q)|^2 \rangle$ is obtained by summing the contribution of each mode. Since the Legendre polynomials behave as $\cos((\nu+1/2)x + \pi/4)$ at small x , the contribution of the mode ν is peaked at $q \simeq \nu/R_{TF}$.

The predictions of Eq. (SM27) may be compared to the one obtained within the Local Density Approximation. Here we focus on the case of thermal equilibrium. We compute the density ripple spectrum injecting the thermal equilibrium value Eq. (SM26) and the mode wave-function Eq. (SM23) into Eq. (SM27). Fig. 3 shows the result for a cloud whose Thomas-Fermi radius fulfills $R_{TF}/l_c = 0.05$, where $l_c = 2\hbar^2 n_p / (mk_B T)$ is the correlation length of the first order correlation function at the center of the cloud, and for a time-of-flight $t_f = 6 \times 10^{-4} m R_{TF}^2 / \hbar$. These parameters are close to the experimental ones. We compared the results with the LDA, together with the analytic formula for homogeneous gases Eq. (SM11) and we find excellent agreement. We also compare with the LDA but using, instead of Eq. (SM11), the approximate approximation Eq. 5 of the main text. We find very good agreement as long as $qR_{TF} < 50$.

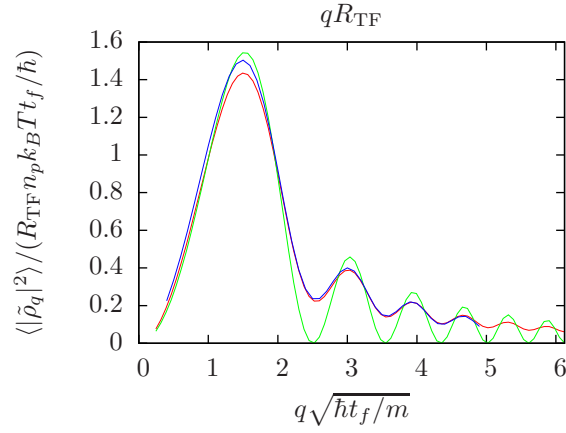


Figure 3: Test of the Local Density Approximation. The plot shows the density ripples spectrum of a gas at thermal equilibrium confined in a harmonic potential. The complete calculation, based on the expansion on the Bogoliubov modes, whose wave functions are given by the Legendre polynomial, is shown in blue. It is in excellent agreement with the spectrum computed within the local density approximation (LDA) shown in red. The further approximation of small wave-vectors, Eq. (5) of the main text, injected into the LDA, is also in good agreement, for wave-vectors fulfilling $qR_{\text{TF}} < 50$. Calculations are done for a Thomas-Fermi radius $R_{\text{TF}}/l_c = 0.05$ and and time-of-flight $t_f = 0.015ml_c^2/\hbar$, where $l_c = 2\hbar^2 n_p / (mk_B T)$ is the correlation length at the center of the cloud. These parameters are close to those of the experimental data.

6 Beyond instantaneous interaction switch off : finite transverse expansion time

In the data presented in the main text, the frequency of the probed longitudinal modes, of the order of cq , is no more than $0.15 \times \omega_{\perp}$. Then, due to the rapid transverse expansion, interactions during the time-of-flight become almost instantaneously negligible and are expected to give only minor corrections to the density ripples spectrum computed for an instantaneous switching off of the interactions. It is nevertheless interesting to estimate their effect. This has already been computed in [3], in the limit $\mu \gg \hbar\omega_{\perp}$ and using time-dependent Bogoliubov equations, *i.e.* equations of motion linearized in density fluctuations and phase gradient. The linearized calculations *a priori* require that density fluctuations stays small. Although in our case density ripples at the end of the time-of-flight have large amplitudes, the Bogoliubov calculations hold for the small q components, which fulfill $ql_c \ll t_f$ and which are considered in our paper. The condition $\mu \gg \hbar\omega_{\perp}$ on the other hand is not verified for the data shown in the main text. We nevertheless believe that the calculations of [3] give a relevant estimation of the effect of interactions during the time-of-flight for our data. From results of [3], we find that the density ripples power spectrum for the small q wavevectors, given by equation (5) of the main text, should be corrected by the factor

$$\mathcal{C} = (\omega_{\perp} t_f)^{-\left(\frac{ck}{\omega_{\perp}}\right)^2}. \quad (\text{SM28})$$

In all experimental situations $\mathcal{C} > 0.95$, which confirm that the effect of interactions during the time-of-flight is small.

7 Effects that may reduce the density ripples power spectrum oscillation amplitude

In this section we investigate two effects responsible for a reduction of the amplitude of the oscillations of \bar{J} (see main text), as compared to the theoretical prediction given by Eq. (6) of the main text. We first consider the effect of the finite ramp time of the interaction strength, which reduces the squeezing of the Bogoliubov modes, as compared to an instantaneous quench. This effect contributes to the reduction of the amplitude by an amount of the order of 10%. We then investigate the reduction of the amplitude induced by the binning of the data with a finite resolution in τ . This effect amounts to an additional reduction of the amplitude by 18%.

7.1 Beyond the instantaneous quench : finite ramp time of the interaction strength

In the experiment, the change of the effective interaction strength is not instantaneous: to ensure the adiabatic following of the transverse motion, we perform a ramp of the transverse oscillation frequency during a time t_r . The finite value of t_r is responsible for a decrease of the induced squeezing of each mode, the squeezing vanishing in the asymptotic limit of very large t_r since then the modes follow adiabatically the modification of the interaction strength. In the following we compute the effect of the ramp on the squeezing of each mode and we use this result to compute the resulting decrease of the oscillation amplitude of \bar{J} .

In order to estimate the effect of the finite ramp time, we will consider a homogeneous gas for simplicity. The Bogoliubov modes are then described by the Hamiltonian of Eq. (1) of the main text, namely

$$H_q = A_q n_q^2 + B_q \theta_q^2. \quad (\text{SM29})$$

We regard the effect of a ramp of ω_{\perp} between the time $t = 0$ and the time t_r , ω_{\perp} going ω_{\perp}^i to $\omega_{\perp}^f = (\kappa + 1)\omega_{\perp}^i$, as depicted in Fig. (4). The coefficient $B_q = n_0 \hbar^2 q^2 / (2m)$ is time-independent, while the coefficient A_q evolves linearly

during the ramp (*i.e.* during time interval $0 < t < t_r$), since it is proportional to c^2 , itself proportional to ω_\perp . Then, the solution of the second order equations describing the evolution of θ_q and n_q during the ramp is given in terms of the Airy functions. In order to investigate the squeezing, it is natural to introduce the reduced variables

$$\begin{cases} \tilde{\theta}_q = \theta_q / \bar{\theta}_q \\ \tilde{n}_q = n_q / \bar{n}_q \end{cases} \quad (\text{SM30})$$

where $\bar{\theta}_q = (A_q(t)/B_q)^{1/4}$ and $\bar{n}_q = (B_q/A_q(t))^{-1/4}$ are the time-dependent widths of the ground state. For given initial values, the values of $\tilde{\theta}_q$ and \tilde{n}_q at the end of the ramp are

$$\begin{pmatrix} \tilde{\theta}_q(t_r) \\ \tilde{n}_q(t_r) \end{pmatrix} = M \begin{pmatrix} \tilde{\theta}_q(0) \\ \tilde{n}_q(0) \end{pmatrix} \quad (\text{SM31})$$

where the matrix M has the following components:

$$\begin{cases} M_{11} = (\kappa + 1)^{-1/4} \pi (-B_i(-\delta^{-2/3})A'_i(-(\kappa + 1)\delta^{-2/3}) + A_i(-\delta^{-2/3})B'_i(-(\kappa + 1)\delta^{-2/3})) \\ M_{22} = (\kappa + 1)^{1/4} \pi (B'_i(-\delta^{-2/3})A_i(-(\kappa + 1)\delta^{-2/3}) - A'_i(-\delta^{-2/3})B_i(-\delta^{-2/3}(\kappa + 1))) \\ M_{21} = (\delta^{-4/3}(\kappa + 1))^{1/4} \pi (-B_i(-\delta^{-2/3})A_i(-\delta^{-2/3}(\kappa + 1)) + A_i(-\delta^{-2/3})B_i(-\delta^{-2/3}(\kappa + 1))) \\ M_{12} = (\delta^{-4/3}(\kappa + 1))^{-1/4} \pi (B'_i(-\delta^{-2/3})A'_i(-\delta^{-2/3}(\kappa + 1)) - A'_i(-\delta^{-2/3})B'_i(-\delta^{-2/3}(\kappa + 1))) \end{cases} \quad (\text{SM32})$$

Here A_i and B_i are the first kind and second kind Airy functions and A'_i and B'_i are their derivatives and $\delta = \kappa/(t_r\omega_q^i)$ is the quench speed normalized to the initial mode frequency (we recall that the quench strength is $\kappa = \omega_\perp^f/\omega_\perp^i - 1$). Under this transformation, the initial isotropic Gaussian distribution transforms into a squeezed distribution, *i.e.* a Gaussian elliptical distribution with a squeezed angle α and ratio between the rms width of the two eigenaxes equal to the squeezing factor S . In order to find α and S , let us compute, for any angle β , the width along the quadrature $\tilde{x}_\beta = \cos(\beta)\tilde{\theta}_q + \sin(\beta)\tilde{n}_q$. Using the fact that the initial state is a thermal equilibrium state fulfilling $\langle \tilde{\theta}_q^2 \rangle_i = \langle \tilde{n}_q^2 \rangle_i = V$ and $\langle \tilde{\theta}_q \tilde{n}_q \rangle_i = 0$, and using the transformation above, we find

$$\langle \tilde{x}_\beta^2 \rangle = V (\cos^2(\beta) (M_{11}^2 + M_{22}^2) + \sin^2(\beta) (M_{21}^2 + M_{12}^2) + 2 \cos(\alpha) \sin(\alpha) (M_{11}M_{21} + M_{22}M_{12})). \quad (\text{SM33})$$

The squeezing angle α is found by imposing $d\langle \tilde{x}_\beta^2 \rangle / d\beta \Big|_{\beta=\alpha} = 0$, which leads to

$$\tan(2\alpha) = -2 \frac{M_{11}M_{21} + M_{22}M_{12}}{M_{21}^2 + M_{12}^2 - M_{11}^2 - M_{22}^2}. \quad (\text{SM34})$$

The most squeezed quadrature is \tilde{x}_α while $\tilde{x}_{\alpha+\pi/2}$ is the most anti-squeezed quadrature and the squeezing factor is $S = \sqrt{\langle \tilde{x}_\alpha^2 \rangle} / \sqrt{\langle \tilde{x}_{\alpha+\pi/2}^2 \rangle}$. It also writes $S = \langle \tilde{x}_\alpha^2 \rangle / V$ since the conservation of the phase-space area ensures $\sqrt{\langle \tilde{x}_\alpha^2 \rangle} \sqrt{\langle \tilde{x}_{\alpha+\pi/2}^2 \rangle} = V$, and it is evaluated injecting $\beta = \alpha$ in Eq. (SM33). Results are shown in Fig. (4) for quench amplitudes $\kappa = 2$ and $\kappa = 4$ as a function of $\omega_q^f t_r$ where ω_q^f is the final frequency of the mode. For very slow modes $\omega_q^f t_r \ll 1$, one recovers the results expected for an instantaneous quench : $\alpha \simeq 0$ and $(S^2 - 1) \simeq \kappa$. For modes of larger frequency, the effect of the ramp is to reduce the squeezing and also to rotate its axis.

The post-quench dynamics results in a breathing of the $\tilde{\theta}_q$ quadrature of amplitude $V(S^2 - 1)/S$. Coming back to the variable of θ_q , the evolution at times $t > t_r$ writes

$$\langle \theta_q^2 \rangle(t) = \langle \theta_q^2 \rangle_i \frac{\sqrt{\kappa + 1}}{S_q} (1 + (S_q^2 - 1) \sin^2(\omega_q^f(t - t_r) + \alpha_q)) \quad (\text{SM35})$$

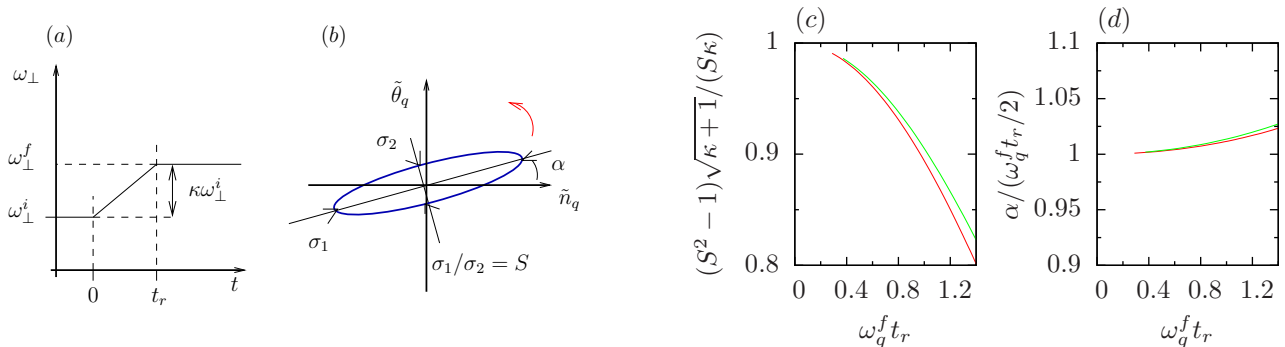


Figure 4: Effect of the interaction strength ramp on the squeezing of longitudinal modes. The time sequence is shown in (a). An example of the phase space distribution at the end of the ramp is shown in (b): the $1/\sqrt{e}$ line of the Gaussian distribution is plotted, the squeezing factor S being the ratio between the rms widths along the anti-squeezed and the squeezed directions. The red arrow shows the direction of rotation under free evolution. Quantitative results are shown in (c) and (d) for a quench strength $\kappa = \omega_{\perp}^f/\omega_{\perp}^i - 1 = 2$ (red lines) and $\kappa = 4$ (green lines). (c) shows $\sqrt{\kappa+1}(S^2-1)/(S\kappa)$, which gives the amplitude of the resulting breathing oscillations normalized to the amplitude for an instantaneous quench (see text), versus $\omega_q^f t_r$ where ω_q^f is the final frequency of the mode. The squeezing angle is shown in (d), normalized by $\omega_q^f t_r/2$.

where the indice q in S and α indicates these quantities depend on q . As seen in Fig. (4), the angle α_q is very close to $\omega_q^f t_r/2$, for moderate values of $\omega_q^f t_r$. Injecting this value into Eq. (SM35), we find that it amounts to shifting the time reference to $t_r/2$. We perform this shift when analyzing the data, in other terms the reduced variable τ is $\tau = cq(t - t_r/2)$.

Let us now consider the evolution of the density-ripples power spectrum $\langle |\tilde{\rho}_q|^2 \rangle(t)$. For small q , $\langle |\tilde{\rho}_q|^2 \rangle(t)$ is proportional to $\langle \theta_q^2 \rangle(t)$ such that the evolution of $\langle |\tilde{\rho}_q|^2 \rangle(t)$ is given by Eq. (SM35). This leads to,

$$J(q, \tau) = \frac{\langle |\tilde{\rho}_q|^2 \rangle(t = \tau/(cq))}{\langle |\tilde{\rho}_q|^2 \rangle_i} = \frac{\sqrt{\kappa+1}}{S_q} (1 + (S_q^2 - 1) \sin^2(\tau)). \quad (\text{SM36})$$

Let us now investigate the quantity $\bar{J}(\tau)$, defined in the main text for experimental data. Here we will assume that the measurement times are spread over $[t_m, t_M]$ and we denote $h(t)dt$ the number of points in the time interval $[t, t + dt]$. The q values are assumed to be equally spaced, as in the case of a Fast Fourier Transform, and only q values in the interval $[q_m, q_M]$ are considered. We assume that $\bar{J}(\tau)$ is obtained by binning in τ the collection of data with a bin size Δ small enough so that, for all measurement times t , $J(q, \tau)$ is about constant in the interval $q \in [\tau/(ct), (\tau + \Delta)/(ct)]$. Then, one has

$$\bar{J}(\tau) = \frac{1}{\int h(t)dt\Delta/(ct)} \int h(t)dt J(q = \tau/(ct), \tau)\Delta/(ct), \quad (\text{SM37})$$

where the integrals are evaluated between t_1 and t_2 , where $t_1 = \text{Max}(t_m, \tau/(cq_m))$ and $t_2 = \text{Min}(t_M, \tau/(cq_M))$. Typically in the experiment small times are sampled more densely than large times. Taking h proportional to $1/t$, we obtain

$$\bar{J}(\tau) = \frac{1}{\int dt/t^2} \int dt J(q = \tau/(ct), \tau)/t^2 = \frac{\int dq J(q, \tau)}{q_2(\tau) - q_1(\tau)}, \quad (\text{SM38})$$

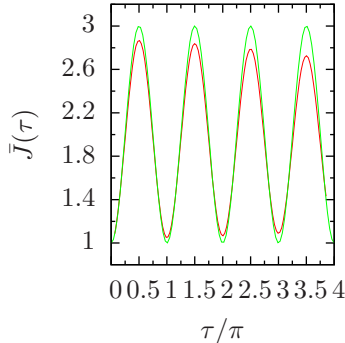


Figure 5: Effect of the finite ramp time of the interaction strength for a homogeneous gas. The expected behavior of \bar{J} (red) is compared to the case of an instantaneous ramp (green). Here we consider a gas of Rubidium atoms at conditions close to the experimental ones. More precisely, the linear density is $n_0 = 630$ atoms per μm , the initial transverse oscillation frequency is $\omega_{\perp} = 2\pi \times 1.5$ kHz, the quench strength is $\kappa = 2$ and the amp time is $t_r = 0.7$ ms. The range of q values used to compute \bar{J} is $q \in [0.1, 0.5]\mu\text{m}^{-1}$ and the range of measurement times is $t \in [t_r/2, 6\text{ms}]$.

where $q_1 = \max(\tau/(c)t_M, q_m)$ and $q_2 = \min(\tau/(c)t_m, q_M)$.

The predicted time evolution of \bar{J} is shown in Fig. (4) for parameters close to that of the experimental data shown in the main text. The amplitude of the first oscillation is decreased by about 10%.

7.2 Finite width of the convolution function used in data processing

The data shown in the inset of Fig. (2) of the main text correspond to a data set with an exceptionally good signal over noise. In general, the spread of the data points corresponding to a given value of τ (and thus corresponding to different times t and wavevectors q) is as large as about 50%. In such conditions, a binning of the data as a function of the reduced time $\tau = cqt$ with a bin size sufficiently large to accommodate many data points is required in order to increase the signal over noise. As describe in the main text, we use a “smooth” binning : we compute the weighted average of the data with a Gaussian cost function of rms width Δ . For very dense set of data, defining the local average value $\tilde{J}(\tau) = \sum_{i, \tau_i \in [\tau, \tau+d\tau]} J_i/d\tau$, where the sum is done on the data set, this weighted averaged corresponds to a convolution of the continuous function \tilde{J} . This convolution reduces the amplitude of the oscillations. To estimate this amplitude reduction, let us disregard the small damping of the oscillations coming from the cloud inhomogeneity (see section 2) and thus consider data which would follow the oscillatory behavior $\tilde{J} = A \sin^2(\tau)$. The smoothing $\bar{J}(\tau) = \int_{-\infty}^{\infty} d\tau' \tilde{J}(\tau') e^{-(\tau'-\tau)^2/(2\Delta^2)}/(\sqrt{2\pi}\Delta^2)$ reduces the amplitude to $A' = Ae^{-2\Delta^2}$. For $\Delta = 0.1\pi$, as used for the data analysis shown in the main text, the amplitude is reduced by 18%.

References

- [1] A. Imambekov, I. E. Mazets, D. S. Petrov, V. Gritsev, S. Manz, S. Hofferberth, T. Schumm, E. Demler, and J. Schmiedmayer. Density ripples in expanding low-dimensional gases as a probe of correlations. *Phys. Rev. A*, 80(3):033604, September 2009.

- [2] S. Dettmer, D. Hellweg, P. Ryytty, J. J. Arlt, W. Ertmer, K. Sengstock, D. S. Petrov, G. V. Shlyapnikov, H. Kreutzmann, L. Santos, and M. Lewenstein. Observation of Phase Fluctuations in Elongated Bose-Einstein Condensates. *Phys. Rev. Lett.*, 87(16):160406, October 2001.
- [3] D. Hellweg, S. Dettmer, P. Ryytty, J. J. Arlt, W. Ertmer, K. Sengstock, D. S. Petrov, G. V. Shlyapnikov, H. Kreutzmann, L. Santos, and M. Lewenstein. Phase fluctuations in BoseEinstein condensates. *Appl Phys B*, 73(8):781–789, December 2001.
- [4] J. N. Fuchs, X. Leyronas, and R. Combescot. Hydrodynamic modes of a one-dimensional trapped Bose gas. *Phys. Rev. A*, 68(4):043610, October 2003.
- [5] M. Olshanii. Atomic Scattering in the Presence of an External Confinement and a Gas of Impenetrable Bosons. *Phys. Rev. Lett.*, 81(5):938–941, August 1998.